

INVESTIGATION OF IMPACT DAMAGE OF TAPERED COMPOSITE LAMINATES

H. ABDULHAMID^{a, b*}, C. BOUVET^a, L. MICHEL^a,
J. ABOISSIERE^b, C. MINOT^b

^a Université de Toulouse ; INSA, UPS, Mines ALBI, ISAE ; ICA (Institut Clément Ader),
ISAE (Institut Supérieur de l'Aéronautique et de l'Espace), 10, avenue Edouard Belin, -BP 54032-
31055 Toulouse Cedex 4

^b Sogeti High Tech, Avenue Escadrille Normandie Niemen, Parc du Millénaire, 31703 BLAGNAC

* e-mail: hakim.abdulhamid@isae.fr

Keywords: impact, ply drop-off, modelling

Abstract

This paper presents a numerical simulation of impact damage of tapered composite laminates. The model is realised in Abaqus Explicit and is capable of reproducing three types of impact damage: matrix cracking, delamination and fibre rupture. An experimental impact test is performed to compare the results with the simulation. Good correlation between experiments and simulations is found in terms of force-displacement response and delamination shape. Finally the model is used to analyse the energy dissipated through damage.

1. Introduction

In structure design, plate or beam thickness needs to be tailored according to local loads in order to optimise material usage. It is achieved by dropping-off plies in the case of composite laminates. However, it is known that ply drop-off can initiate damage like matrix crack and delamination [1]–[3]. This vulnerability results from the material discontinuities due to local curvature of continuous plies and resin pockets. Furthermore, composite laminates show low tolerance to impact. Even at low energy, damage propagates far beyond the impact point which leads to significant reduction of the residual strength in compression [4], [5]. The complexity of the impact phenomenon and the lack of robust method for damage tolerance prediction have forced the industries to run expensive experimental campaigns and oversize their structure. Many authors have contributed to the development of numerical model of damage of composites structures. For example, Ladevèze et al. [6], [7] considered that the meso-scale characterized by ply thickness is the proper scale to reproduce the type of damage encountered during impact. Both Continuum Damage Mechanics and Fracture Mechanics are commonly used to pilot the propagation of damage [8], [9]. Ply drop-off has been largely numerically studied in static [10], [11] but there has been no attempt yet to run a simulation of impact in presence of ply drop-off.

This work is a continuation of the effort of Bouvet et al. [12]–[14] to develop a predictive numerical model for the impact of composite laminates. Their approach named as Discrete

Ply Modelling has already provided good correlation for the simulation of impact of plain laminates [13]. Ply drop-off adds new difficulty to the simulation but at the same time constitutes a good test case for the robustness of the model. In this study, an impact test is realised on a tapered laminate. Then, the test is simulated using the DPM approach. Finally, the numerical data is used to analyse the impact damage mechanism.

2. Experimental study

The study is performed on a specimen with a thickness changing from 4 mm in the thin section to 6 mm in the thick section. In the thin section, the stacking sequence is $[45_2, -45_2, 0_2, 90_2]_s$. Then, 4 groups of plies, all oriented in the 0° direction are added in the middle of the specimen which gives a layup of $[45_2, 0_2, -45_2, 0_2, 90_2, 0_2]_s$ in the thick section. The groups of plies are dropped-off in a staggered way with step spacing of 1.5 mm (table 1). The length of the thin section is 125 mm as shown in figure 1. The specimen is made of carbon/epoxy T700/M21 material and has a rectangular dimension of 250 x 100 mm².

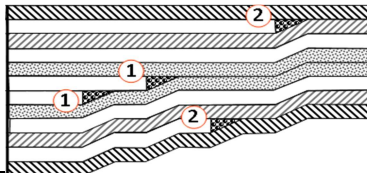
specimen A ^T		$[45_2$	0_2	-45_2	0_2	90_2	$0_2]_s$	
termination order	-	2 nd	-	-	-	-	1 st	

Table 1 Specimens layup

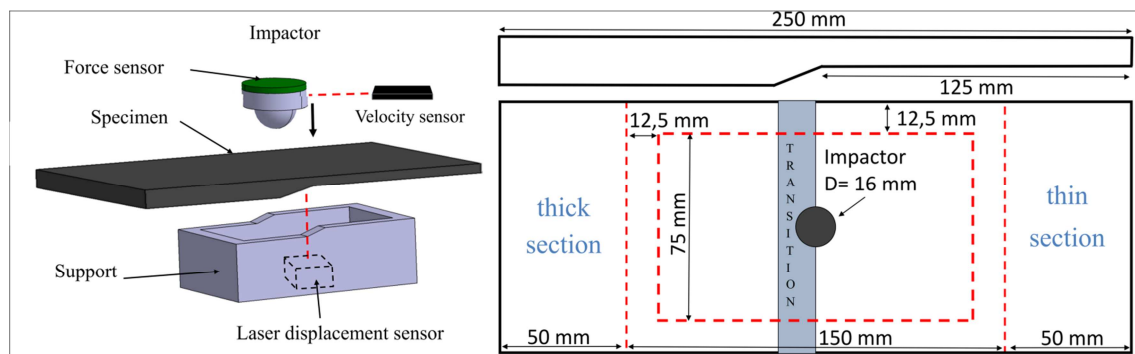


Figure 1: Impact boundary conditions and specimen geometry

The impact tests are performed on a dropped weight testing rig with an impactor mass of 4 kg. The indenter has a hemispherical shape of 16 mm-diameter. Impact boundary conditions are similar to the Airbus standard AITM 1-0010; specimen is simply supported by a window of 125 x 75 mm² dimensions (figure 1). The impact target is at the centre of the specimen.

3. Numerical modelling

The impact is simulated with the non-linear dynamic explicit solver of Abaqus v6.11. A detailed description of the concept of the model is available in [13], [15]. The laminate is modelled at a meso-scale level where each sequence of plies of the same orientation is represented by one element in the thickness. The meshing strategy defined as the Discrete Ply Modelling is inspired by the three major impact damage (matrix cracking, delamination and fibre rupture). In this approach, each group of plies with the same orientation is modelled by strips of 3D volume elements (C3D8) oriented in the ply direction. The strips are then

connected by zero thickness intra-ply cohesive elements (COH3D8) in the transverse direction (figure 2a). Those cohesive elements are there to represent the discontinuity created by trans-laminar matrix cracking of the ply. Then, the discrete ply model is stacked one on top of the other with zero thickness inter-ply cohesive elements (COH3D8) to model delamination. The element size for 0° and 90° plies is 1.5 x 1.5 mm². The use of delamination elements to connect two neighbour plies imposes the nodes of volume elements to be coincident on either sides of the interface. As a result the shape of 45° and -45° volume elements are distorted (figure 2b).

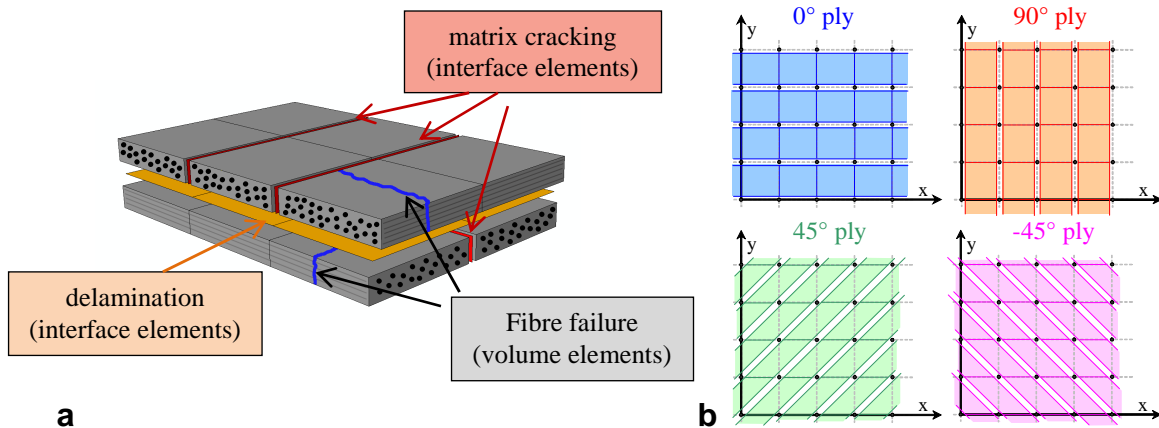


Figure 2: a- Element choice for the modelling of damage, b- ply meshing

Figure 3 describes the modelling of the transition region. In this example, plies 1 and 3 are continuous and ply 2 is dropped-off. The delamination elements connected to the dropped-off ply are also terminated at the same point. Then, in the thin section, a new set of delamination elements is created between the continuous plies. The resin pocket is not filled with any material in the model. There are no volume elements for the resin or cohesive elements to bond the continuous plies. From a structure point of view, it is as if the resin pocket area is delaminated before the impact. This choice has already been used for static simulation in the literature [11]. It is even more justified in the case of impact simulation since the emphasis is more on the propagation of delamination than its initiation. Therefore, the need to implement special element for the resin pocket is less important in this study.

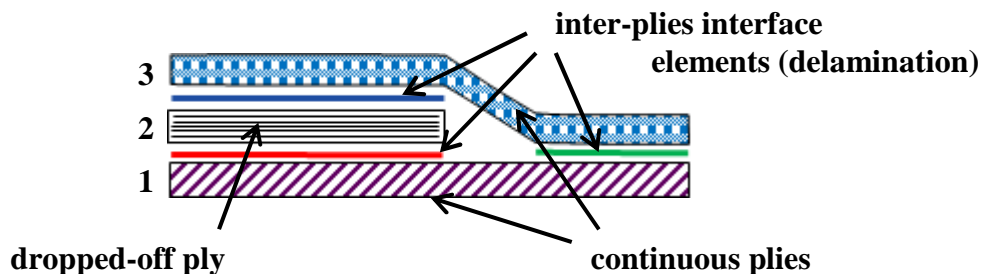


Figure 3: Modelling of the transition region

ρ	E_1^T	E_1^C	E_2	G_{12}	ν_{12}	σ_2^{T0}	σ_{12}^0
1600 kg/m ³	130 GPa	100 GPa	7.7 GPa	4.8 GPa	0.33	48 MPa	88 MPa

Table 2 Mechanical properties of T700GC/M21 unidirectional ply

Elements material laws are defined in a VUMAT subroutine. The behaviour of all elements remains linear before the onset of any damage. The response of the laminate is therefore governed by the orthotropic property of the material (table 2). In the model, matrix cracking is represented by the failure of intra-ply interface elements. A quadratic criterion computed in the volume elements Eq.(1), triggers the failure of a neighbour interface element. Delamination presented in the inter-ply interface elements is computed as a linear coupling of three modes Eq.(2): inter-laminar opening (mode I), sliding (mode II) and tearing (mode III) (figure 4a). There is no parameter to account for the interaction between matrix cracking and delamination. It is directly achieved by the discontinuity created by the trans-laminar opening.

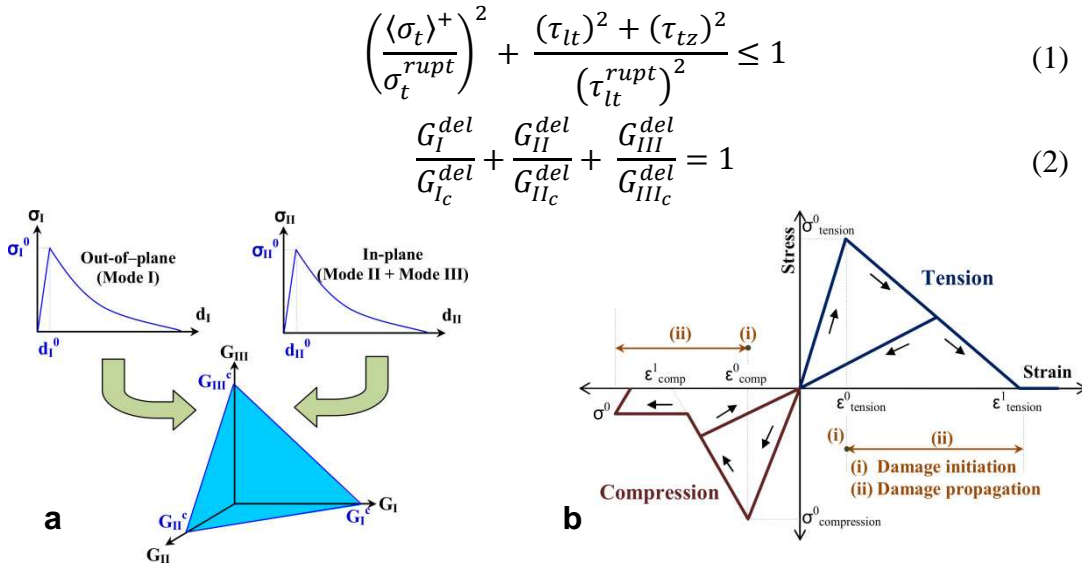


Figure 4 Material laws **a-** linear coupling delamination, **b-** fibre failure

The initiation of fibre rupture is defined by the maximum strain inside the element which is obtained by extrapolating the strain at nodes. Then, the damage propagation is computed so that the critical energy release rate of the fibre is dissipated inside the element throughout the eight integration points. The energy dissipated due to fibre rupture is non-mesh sensitive as presented in Eq.(3) [16].

$$\sum_{i=1}^8 \frac{V}{8} \cdot \int_0^{\varepsilon_1^i} \sigma_l^i \cdot d\varepsilon_l^i = S \cdot G_{Ic}^{fibre} \quad (3)$$

Where σ_l^i , ε_l^i and ε_1^i are respectively the longitudinal stress, the longitudinal strain the longitudinal failure strain at the integration point i . V and S are the volume and the cross section normal to the fibre direction of an element and G_{Ic}^{fibre} is the critical energy release rate of the fibre. The same response is also used in compression with an addition of a crushing plateau of -270 MPa (figure 4b). The material failure property used in the simulation is given in table 3.

Fibre failure				delamination	
ε_1^{T0}	ε_1^{C0}	$G_{Ic}^{fibre, trac}$ (N/mm)	$G_{Ic}^{fibre, comp}$ (N/mm)	G_{Ic}^{del} (N/mm)	G_{IIc}^{del} (N/mm)
0.016	-0.0125	133	40	0.52	1.66

Table 3: Failure mechanism material properties of T700/M21

4. Comparison of numerical simulation with experiment

In this study, the value of impact energy was chosen high enough (30J) to create three types of damage: matrix cracking, delamination and fibre rupture. This can be clearly observed in the force-displacement curve (figure 5). This curve provides global information regarding the damage scenario. For example, in this case it gives the contact force that triggers delamination and also indicates the existence of important fibre rupture during the impact. Therefore, the various damage law implemented in the model can be tested.

The comparison of the force-displacement curves between experiment and simulation shows good aptitude of the model to predict the global damage scenario. First, the initiation of delamination when the contact force is around 3.75 kN is well estimated. It is important to notice that the absence of delamination interface elements at the resin pocket in the model does not underestimate this value. Then, the model does reproduce quite well the propagation of delamination throughout the impact. Finally, an important fibre rupture appearing at 8.5 kN is also well predicted in the simulation. The force drop is more important in the simulation compared to the experiment.

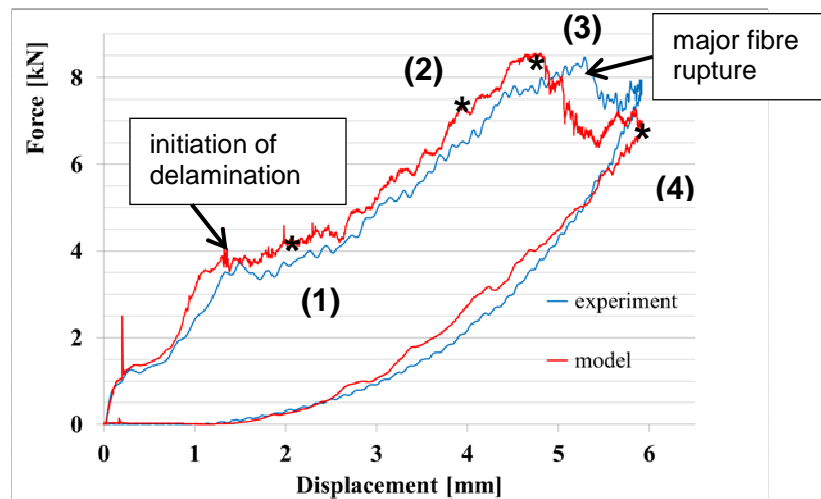


Figure 5: Comparison of impact force vs displacement curves

Delamination (figure6b) of the plate is obtained from C-scan performed from the impacted side. Also, data from the numerical model is processed with the same colour spectrum to obtain the predicted delamination map (figure6c). Due to the thickness change on either sides of the transition region, it is possible that an interface is represented by two different colours. The delamination profile provided in figure6a simplifies the identification of the delaminated interfaces. Note that, regardless of the presence of ply drop-off, the direction of propagation of delamination still follows the direction of the lower ply. Also, the largest delaminated interfaces are between continuous plies. Globally, the predicted morphology of delamination

is in good agreement with the experiment. The first and the last interfaces are a little bit overestimated though.

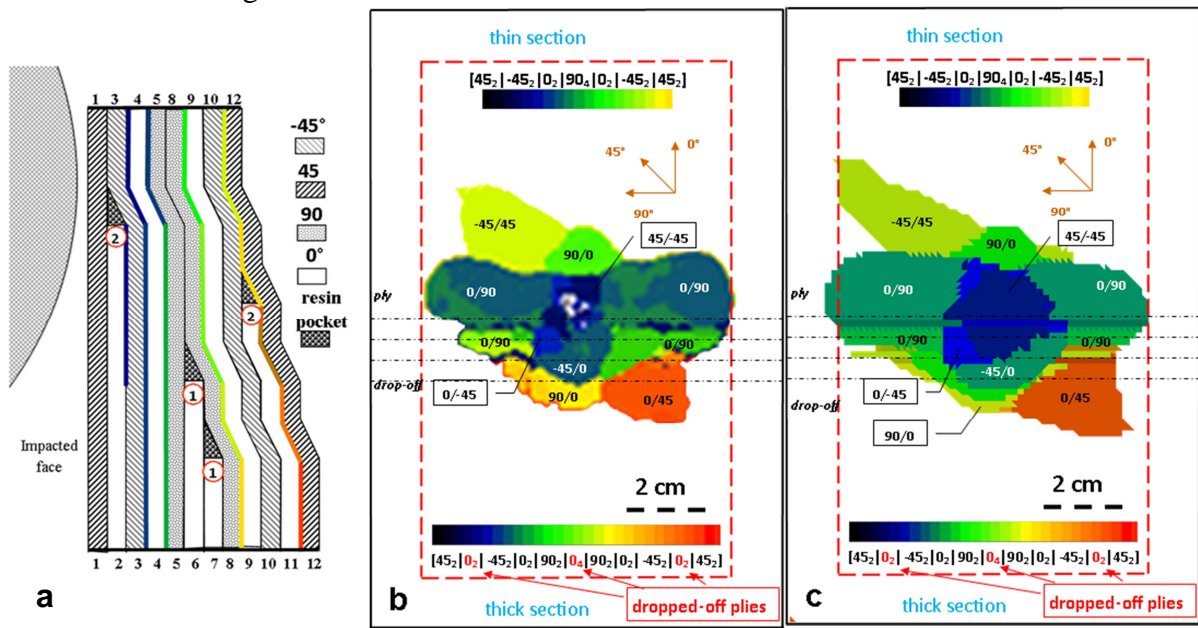


Figure 6: Comparison of delamination morphology **a**-profile **b**- experiment and **c**- simulation

Figure 7 shows the progression of delamination throughout the impact. The images are taken at the four points located in the force-displacement curve. They correspond respectively to an out-of-plane displacement of 2.25 mm, 4.10 mm, 4.80 mm and 5.90 mm. Three important phases in the delamination process can be distinguished. Firstly, in figure 7-(1), delaminations propagate in all directions with more or less the same rate. Secondly, the propagation toward the thick section is slowed down and at the same time the propagation rate in the transverse direction accelerates (figure 7-(2) and 7-(3)). Thirdly, the onset of fibre rupture stops the propagation in the transverse direction and triggers the propagation of the 0/45 and -45/45 out-most interfaces (figure 7-(4)).

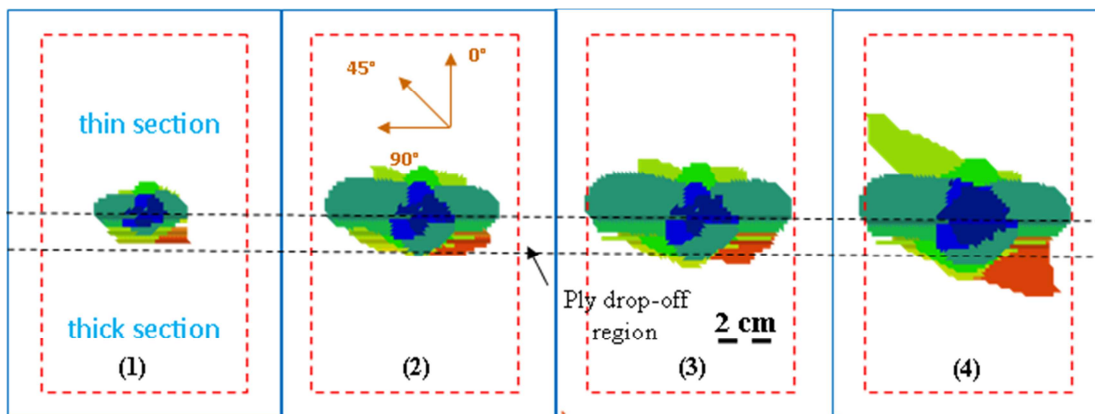


Figure 7: Progression of delamination (1): 2.25 mm, (2): 4.10 mm, (3): 4.80 mm, (4): 5.90 mm

Regarding the energy distribution, in the experiment, 18.7 J of the 30 J is transmitted to the specimen. A large part of this energy is dissipated through damage but there is still some part which cannot be separated from the experimental data that is transformed into kinetic energy inside the specimen. In the simulation, 16.2 J is dissipated throughout damage created during the impact. 55 % of this energy is dissipated in delamination and 45% in fibre rupture. The energy dissipated in the model is slightly lower compared to the experiment because it does

not take into account the energy dissipated in matrix cracking. Figure 8 presents the contribution of each mode in the delamination propagation. In the centre of the specimen, the propagation is predominately in mode II and III while it is in mixed mode I, II and III near to the edges.

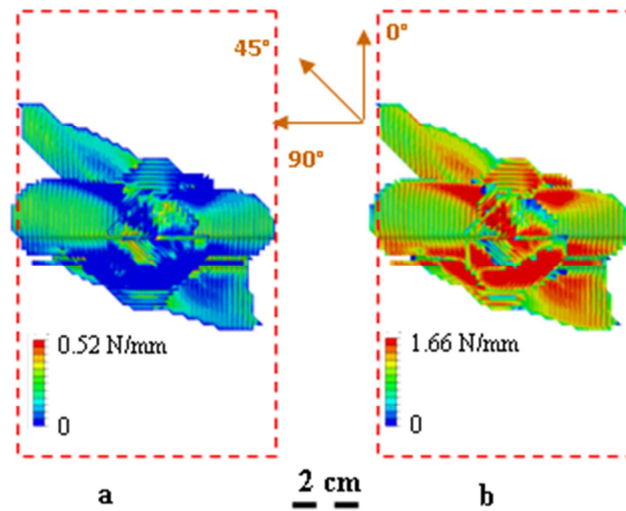


Figure 8: Distribution of energy dissipated in delamination (a): mode I, (b): mode II and III

5. Conclusion

This study constitutes the first attempt to model the impact of a tapered laminate composite in the literature. The Discrete Ply Model approach which has already provided good results in the case of plain laminates was used. No specific modelling of the resin pocket was required in order to achieve good correlation with the experiment. Both the force-displacement curve and delamination morphology are well predicted by the model besides the presence of material discontinuity of the ply drop-off and also the existence of different phases of delamination propagation. Those results demonstrate that the DPM approach mixed with the material law used presents good robustness for the prediction of impact damage.

This study will be further pursued to integrate the CAI into the model to simulate the damage tolerance of this type of specimen. New type of stacking, with different orientation dropped-off plies will also be studied.

References

- [1] C. A. Steeves and N. A. Fleck, "Compressive strength of composite laminates with terminated internal plies," *Compos. Part A Appl. Sci. Manuf.*, vol. 36, no. 6, pp. 798–805, Jun. 2005.
- [2] A. Weiss, W. Trabelsi, L. Michel, J. J. Barrau, and S. Mahdi, "Influence of ply-drop location on the fatigue behaviour of tapered composites laminates," *Procedia Eng.*, vol. 2, no. 1, pp. 1105–1114, Apr. 2010.
- [3] M. R. Wisnom, R. Dixon, and G. Hill, "Delamination in asymmetrically tapered composites loaded in tension," *Compos. Struct.*, vol. 35, no. 3, pp. 309–322, Jul. 1996.
- [4] H. Kaczmarek and S. Maison, "Comparative ultrasonic analysis of damage in CFRP under static indentation and low-velocity impact," *Composites Science and Technology*, vol. 51, pp. 11–26, 1994.

- [5] S. Petit, C. Bouvet, A. Bergerot, and J.-J. Barrau, "Impact and compression after impact experimental study of a composite laminate with a cork thermal shield," *Compos. Sci. Technol.*, vol. 67, no. 15–16, pp. 3286–3299, Dec. 2007.
- [6] P. Ladevèze and O. Allix, "Basic aspect of damage meso-modelling," in *Engineering Mechanics Proceeding of the Ninth Conference.*, 1992, pp. 373–376.
- [7] O. Allix, "A composite damage meso-model for impact problems," *Compos. Sci. Technol.*, vol. 61, no. 15, pp. 2193–2205, Nov. 2001.
- [8] B. G. Falzon and P. Apruzzese, "Numerical analysis of intralaminar failure mechanisms in composite structures. Part I: FE implementation," *Compos. Struct.*, vol. 93, no. 2, pp. 1039–1046, Jan. 2011.
- [9] L. Iannucci and J. Ankersen, "An energy based damage model for thin laminated composites," *Compos. Sci. Technol.*, vol. 66, no. 7–8, pp. 934–951, Jun. 2006.
- [10] H. S. Kim, S. Y. Rhee, and M. Cho, "Simple and efficient interlaminar stress analysis of composite laminates with internal ply-drop," *Compos. Struct.*, vol. 84, no. 1, pp. 73–86, Jun. 2008.
- [11] K. He, S. Hoa, and R. Ganesan, "The study of tapered laminated composite structures: a review," *Compos. Sci. Technol.*, vol. 60, no. 14, pp. 2643–2657, Nov. 2000.
- [12] E. A. Abdallah, C. Bouvet, S. Rivallant, B. Broll, and J.-J. Barrau, "Experimental analysis of damage creation and permanent indentation on highly oriented plates," *Compos. Sci. Technol.*, vol. 69, no. 7–8, pp. 1238–1245, Jun. 2009.
- [13] N. Hongkarnjanakul, C. Bouvet, and S. Rivallant, "Validation of low velocity impact modelling on different stacking sequences of CFRP laminates and influence of fibre failure," *Compos. Struct.*, vol. 106, pp. 549–559, Dec. 2013.
- [14] C. Bouvet, S. Rivallant, and J. J. Barrau, "Low velocity impact modeling in composite laminates capturing permanent indentation," *Compos. Sci. Technol.*, vol. 72, no. 16, pp. 1977–1988, Nov. 2012.
- [15] C. Bouvet, B. Castanié, M. Bizeul, and J.-J. Barrau, "Low velocity impact modelling in laminate composite panels with discrete interface elements," *Int. J. Solids Struct.*, vol. 46, no. 14–15, pp. 2809–2821, Jul. 2009.
- [16] P. Bazant and H. B. Oh, "Crack band theory for fracture of concrete," vol. 16, pp. 155–77, 1983.